THE JOURNAL OF BIOLOGICAL CHEMISTRY VOL. 287, NO. 10, pp. 7246–7255, March 2, 2012

Molecular Identification of Hydroxylysine Kinase and of Ammoniophospholyases Acting on 5-Phosphohydroxy-L-lysine and Phosphoethanolamine*

Received for publication, November 15, 2011, and in revised form, January 11, 2012 Published, JBC Papers in Press, January 12, 2012, DOI 10.1074/jbc.M111.323485

Maria Veiga-da-Cunha[‡1], **Farah Hadi**[‡], **Thomas Balligand**[‡], **Vincent Stroobant**[§], **and Emile Van Schaftingen**[‡2]

From the [‡]*Laboratory of Physiological Chemistry and the* [§]*Ludwig Institute for Cancer Research, de Duve Institute and Université Catholique de Louvain, B-1200 Brussels, Belgium*

Background: Vertebrate genomes encode AGXT2L1 and AGXT2L2, two related, pyridoxal-phosphate dependent enzymes of unknown function.
Results: Comparison with bacterial genomes suggested that AGXT2L1 and AGXT2L2 are ammoniophospholyases functionally related with AGPHD1. The three recombinant proteins were produced and studied.
Conclusion: AGXT2L1 is *O*-phosphoethanolamine phospholyase; AGXT2L2 is 5-phosphohydroxy-L-lysine phospholyase; AGPHD1 is 5-hydroxylysine kinase.
Significance: These molecular identifications will help explain some specific neurometabolic diseases.

The purpose of the present work was to identify the catalytic activity of AGXT2L1 and AGXT2L2, two closely related, putative pyridoxal-phosphate-dependent enzymes encoded by vertebrate genomes. The existence of bacterial homologues (40–50% identity with AGXT2L1 and AGXT2L2) forming bi- or trifunctional proteins with a putative kinase belonging to the family of aminoglycoside phosphotransferases suggested that AGXT2L1 and AGXT2L2 acted on phosphorylated and aminated compounds. Vertebrate genomes were found to encode a homologue (AGPHD1) of these putative bacterial kinases, which was therefore likely to phosphorylate an amino compound bearing a hydroxyl group. These and other considerations led us to hypothesize that AGPHD1 corresponded to 5-hydroxy-L-lysine kinase and that AGXT2L1 and AGXT2L2 catalyzed the pyridoxal-phosphate-dependent breakdown of phosphoethanolamine and 5-phosphohydroxy-L-lysine. The three recombinant human proteins were produced and purified to homogeneity. AGPHD1 was indeed found to catalyze the GTP-dependent phosphorylation of 5-hydroxy-L-lysine. The phosphorylation product made by this enzyme was metabolized by AGXT2L2, which converted it to ammonia, inorganic phosphate, and 2-aminoadipate semialdehyde. AGXT2L1 catalyzed a similar reaction on phosphoethanolamine, converting it to ammonia, inorganic phosphate, and acetaldehyde. AGPHD1 and AGXT2L2 are likely to be the mutated enzymes in 5-hydroxylysinuria and 5-phosphohydroxylysinuria, respectively. The high level of expression of AGXT2L1 in human brain, as well as data in the literature linking AGXT2L1 to schizophrenia and bipolar disorders, suggest that these diseases may involve a perturbation of brain phosphoethanolamine metabolism. AGXT2L1 and AGXT2L2, the first ammoniophospholyases to be identified, belong to a family of aminotransferases acting on ω-amines.

Pyridoxal-phosphate (PLP)[3]-dependent enzymes catalyze a series of reactions, mostly on amino compounds, that include the transfer of amine, the decarboxylation and racemization of amino acids, and β- and γ-elimination reactions on amino acids (1). A recent review reports more than 50 human enzymes or putative enzymes using PLP as a cofactor (2). Many of these enzymes have a known function, yet the reaction catalyzed by a few of them is still unknown. This is particularly the case for mammalian AGXT2L1 (AGXT2-like 1) and AGXT2L2 (AGXT2-like 2), two enzymes that share ≈36% sequence identity with mammalian AGXT2 (alanine:glyoxylate aminotransferase 2). AGXT2 is a member of the aminotransferase III subfamily (as defined in the Pfam database (3)), which mostly comprises enzymes that catalyze transamination on ω-amines. It catalyzes the pyruvate-dependent conversion of D-β-aminoisobutyrate, a breakdown product of thymine, to methylmalonate semialdehyde (4). Unlike AGXT2, AGXT2L1 and AGXT2L2 did not act as transaminases (5).

The purpose of the present work was to identify the function of AGXT2L1 and AGXT2L2. We show how bacterial homologues of these proteins, because of their association with a kinase of unknown function (homologous to a protein named AGPHD1), led us to hypothesize that AGXT2L1 and AGXT2L2 are ammoniophospholyases acting on phosphoethanolamine (*P*EtN) and (5*R*)-5-phosphohydroxy-L-lysine (5*P*Hyl).

* This work was supported by grants from the Fonds National de la Recherche Scientifique and Fonds de la Recherche Scientifique Médicale, the Center of Excellence des Désordres Inflammatoires dans les Affections Neurologiques Programme of the Région Wallonne, and ASCO Industries.

[1] Chercheur Qualifié of the Belgian Fonds National de la Recherche Scientifique. To whom correspondence may be addressed: de Duve Institute, Ave. Hippocrate box B1.75.08, B-1200 Brussels, Belgium. Tel.: 32-2-764-75-59; Fax: 32-2-765-75-98; E-mail: maria.veiga@uclouvain.be.

[2] To whom correspondence may be addressed: de Duve Institute, Ave. Hippocrate box B1.75.08, B-1200 Brussels, Belgium. Tel.: 32-2-764-75-59; Fax: 32-2-765-75-98; E-mail: emile.vanschaftingen@uclouvain.be.

[3] The abbreviations used are: PLP, pyridoxal-phosphate; 2-AASA, 2-aminoadipate semialdehyde; 5Hyl, (5*R*)-5-hydroxy-L-lysine; *P*EtN, phosphoethanolamine; 5*P*Hyl, (5*R*)-5-phosphohydroxy-L-lysine; contig, group of overlapping clones.

TABLE 1

Sequence of the primers used for the amplification and cloning of human AGXT2L1, AGXT2L2, and AGPHD1 their expression plasmid

The nucleotides that correspond to the coding sequences are in capital letters, and the restriction sites added are in lowercase letters and underlined.

Primer	Sequence	Restriction site	Plasmid	Protein expressed
hAGXT2L1-NdeI	5′-ccccatATGTGCGAGCTGTACAGTAAG-3′	NdeI	pET24a or pET28a	N- and C-tagged His_6AGXT2L1
bis28hAGXT2L1-NotI	5′-gcgcggccgcTCATGTCTTGAGCCTCTTACTG-3′	NotI	pET28a	N-tagged His_6AGXT2L1
bis24hAGXT2L1-NotI	5′-aagcggccgcTGTCTTGAGCCTCTTACTGAGC-3′	NotI	pET24a	C-tagged His_6AGXT2L1
S-AGXT2L1[a]	5′-GCAGACTCATCCAGTGCTTA-3′			
AS-AGXT2L1[a]	5′-GCTGGAGGAATTATTTGTCCG-3′			
hAGXT2L2-NdeI	5′-ccacatATGGCCGCAGACCAGCGC-3′	NdeI	pET24a or pET28a	N- and C-tagged His_6AGXT2L2
28hAGXT2L2-NotI	5′-cagcggccgcTTAGGGCTGGAGCCTCAGC-3′	NotI	pET28a	N-tagged His_6AGXT2L2
24hAGXT2L2-NotI	5′-ggggcggccgcGGGCTGGAGCCTCAGCGT-3′	NotI	pET24a	C-tagged His_6AGXT2L2
hAGPHD1-NdeI	5′-gaccatATGTCAAGTGGAAACTATCAGC-3′	NdeI	pET28a	N-tagged His_6AGPHD1
bishAGPHD1-NotI	5′-gcgcggccgcTCACATGGAGATCCCAGATTC-3′	NotI		
hAGPHD1-NcoI[b]	5′-gaccccATG**G**CAAGTGGAAACTATCAGCAG-3′	NcoI	pET28a	C-tagged His_6AGPHD1
bishAGPHD1-NotI (without stop)	5′-gcgcggccgcCATGGAGATCCCAGATTCATAG-3′	NotI		

[a] Primers corresponding to internal sequences of the AGXT2L1 cDNA that were combined with external ones to amplify the 5′ and the 3′ regions of the AGXT2L1 coding sequence. The overlapping PCR products were then used to obtain the full-length coding sequence using the corresponding external primers.

[b] To create a NcoI restriction site, we replaced a T in the second codon by a G (shown in bold). In addition to the C-terminal His_6 tag, this results in S2A replacement in the expressed recombinant protein.

*P*EtN, a component and a precursor of phospholipids, is produced through phosphorylation of free ethanolamine by ethanolamine kinase (6, 7), through the breakdown of phosphatidylethanolamine by phospholipase C (8, 9), or through aldolytic cleavage of sphinganine-1-phosphate by sphinganine-1-phosphate lyase (10). *P*EtN is metabolized by a PLP-dependent enzyme, of unknown molecular identity, that catalyzes the elimination of inorganic phosphate (P_i) and ammonia, leading to the formation of acetaldehyde (11). Initially described in mammalian tissues, this activity appears to be present also in bacteria, such as *Erwinia carotovora* (now called *Pectobacterium carotovorum var. atrosepticum*) (12). A distinct PLP-dependent ammoniophospholyase is involved in the breakdown of 5*P*Hyl in mammalian tissues, leading to the formation of ammonia, 2-aminoadipate semialdehyde (2-AASA) and P_i (13). 5*P*Hyl is produced through the phosphorylation of (5*R*)-5-hydroxy-L-lysine (5Hyl), a breakdown product of collagen, by a GTP-dependent kinase (14). The molecular identity of the kinase and of the ammoniophospholyase that are involved in the metabolism of 5Hyl were unknown before we started this work. We describe here the database searches and the experiments that led us to provide the molecular identification of *P*EtN phospholyase and of the two enzymes involved in 5Hyl metabolism in mammalian tissues.

EXPERIMENTAL PROCEDURES

Materials—5Hyl and 5-hydroxy-DL-lysine were from Sigma, allysine ethylene acetal was from Aldrich, and HisTrap HP columns were from Qiagen. Optimase polymerase was from Transgenomics. pET expression plasmids were from Novagen. Yeast alcohol dehydrogenase, beef liver glutamate dehydrogenase, rabbit muscle pyruvate kinase, and lactate dehydrogenase were from Roche Applied Science.

Cloning, Overexpression and Purification of Recombinant Proteins—The open reading frames of human AGXT2L1, AGXT2L2, and AGPHD1 were PCR-amplified using human cDNA (brain for AGXT2L1 and kidney for AGXT2L2 and AGPHD1) as a template. The PCR fragments obtained in the presence of 1 M betaine using the Optimase polymerase were purified, digested with the appropriate restriction enzymes (restriction site included in the primers), and ligated into an adequately restricted expression plasmid. For AGXT2L1 and AGXT2L2, the PCR fragments permitting the expression of fusion proteins with an N-terminal His_6 tag were cloned in pET28a and those with a C-terminal His_6 tag were cloned in pET24a after incubation with NdeI and NotI restriction enzymes. For AGPHD1, N- and C-terminal fusion proteins were expressed using pET28a plasmids harboring the PCR fragments corresponding to AGPHD1 cloned in NdeI/NotI- or NcoI/NotI-restricted plasmids, respectively. When proteins were fused with a C-terminal His_6 tag, the sequence of the primers used in the PCR removed the natural STOP codon. Table 1 shows the sequence of the primers used in the PCRs. The ligated plasmids were amplified in *Escherichia coli* XL1 blue, and the positive clones were checked by sequencing to rule out any PCR errors and finally transformed in *E. coli* BL21(DE3). All of the expression experiments were in 2-liter flasks containing 500 ml of culture media for 18 h (AGXT2L1 and AGXT2L2) or 72 h (AGPHD1) in the presence of 0.4 mM isopropyl β-D-thiogalactoside. AGXT2L1 and AGXT2L2 with a N- or a C-terminal His_6 tag were expressed in M9 medium at 20 °C. In the case of the more instable AGPHD1, we expressed the C-terminally tagged protein in M9 medium at 16 °C.

Preparation of bacterial extracts (25 ml) and their centrifugation was as described previously (15) with two exceptions in the composition of the extraction buffer: 1) for the bacteria expressing AGXT2L1, the extraction buffer contained 1 mM phenylmethylsulfonyl fluoride to reduce proteolysis at the C-terminal end and 2) 0.3 M NaCl was added to all buffers during extraction and purification of AGPHD1 to prevent precipitation of this protein.

The supernatants (20 ml) were supplemented with 0.3 M NaCl, diluted 3-fold in buffer A (50 mM $NaPO_4$, pH 8.0, 0.3 M), and applied onto a 1-ml HisTrap HP column (Ni^{2+} form) previously equilibrated with buffer A. The column was washed with buffer A containing 15 mM imidazole (≈25 ml), and the retained proteins were eluted with a 20-ml linear imidazole (0.015–0.3 M) gradient in buffer A. Protein elution with imidazole and the purity of the fractions was analyzed by SDS-PAGE. All of the recombinant proteins showed the expected size (≈43 kDa for AGPHD1, ≈57 kDa for AGXT2L1, and ≈51 kDa for AGXT2L2, including the His_6 tag). Three to four selected fractions were pooled, concentrated, desalted as previ-

ously described (16), and stored at −70 °C in 25 mM Hepes, pH 7.1, containing 1 $\mu g \cdot ml^{-1}$ leupeptin and antipain, 0.01, 0.1, or 0.3 M NaCl (for AGXT2L2, AGXT2L1, or AGPHD1, respectively) and 10% glycerol. Protein concentration was estimated by measuring A_{280} and assuming molar absorptivities of 31143 (AGXT2L1), 35090 (AGXT2L2), and 43445 (AGPHD1) $M^{-1} \cdot cm^{-1}$. From 1 liter of culture, we obtained on average 10–15 mg of pure protein.

Purified AGXT2L1 and AGXT2L2 were yellow, suggesting that they did indeed bind PLP. Because the position of the His_6 tag did not interfere with the kinetic properties that we investigated, we chose to report the results obtained for AGPHD1 and AGXT2L1 tagged at the C-terminal end and for AGXT2L2 tagged at the N-terminal end, based on a higher purification yield obtained for these fusion proteins.

Measurement of 5Hyl-kinase and PEtN-phospholyase Activities—The 5Hyl-kinase activity of AGPHD1 was assayed spectrophotometrically at 30 °C using a pyruvate kinase/lactate dehydrogenase-coupled assay. The assay mixture (0.6 ml) contained 25 mM Hepes, pH 7.1, 0.15 mM NADH, 0.25 mM phosphoenolpyruvate, 1 mM dithiothreitol, 25 mM KCl, 0.2 mM GTP-Mg or 2 mM ATP-Mg, 5 mM $MgCl_2$, 8 μg of lactate dehydrogenase and pyruvate kinase, and the indicated concentrations of 5Hyl (the physiological form of hydroxylysine found in collagen) and ≈2.5 $\mu g \cdot ml^{-1}$ of purified recombinant human AGPHD1. When necessary, other substrates were tested as indicated under "Results."

*P*EtN-phospholyase activity of AGXT2L1 was routinely assayed spectrophotometrically by monitoring the production of acetaldehyde. The activity was measured at 30 °C in a final volume of 0.6 ml containing 50 mM triethanolamine, pH 7.4, 0.15 mM NADH, 5 μM PLP, 1 mM EGTA, 0.5 $mg \cdot ml^{-1}$ bovine serum albumin, 0.2 $mg \cdot ml^{-1}$ desalted yeast alcohol dehydrogenase, and 28 $\mu g \cdot ml^{-1}$ purified recombinant human AGXT2L1.

Synthesis and Purification of [^{31}P] and [^{32}P]5PHyl—[^{32}P]*5P*Hyl was produced by the phosphorylation of 5Hyl with purified recombinant human AGPHD1. Practically, 0.1 ml of 25 mM Hepes, pH 7.5, containing 5 mM $MgCl_2$, 25 mM KCl, 1 mM DTT, 0.5 mM 5Hyl, 5 μM ATP-Mg, and 1.5×10^8 cpm [γ-^{32}P]ATP was incubated at 30 °C in the presence of 5 μg of AGPHD1. After 30 min, the reaction was stopped (5 min at 80 °C), and [^{32}P]*5P*Hyl was separated from other radioactive compounds present in the reaction mixture ([^{32}P]P_i and [γ-^{32}P]ATP) using anion exchange chromatography. At neutral pH, the resin retained negatively charged molecules (P_i and ATP), whereas *5P*Hyl was eluted in the washing fractions. The reaction mixture was diluted 10-fold in buffer A (10 mM Hepes, pH 7.5) and loaded onto a 1-ml DOWEX AG1X8 column equilibrated in the same buffer and washed with 9 ml of buffer A to recover radiolabeled *5P*Hyl (which contained 73% of total radioactivity). The nonradioactive *5P*Hyl was prepared in a similar way by incubating 1 ml of 50 mM Hepes, pH 7.5, 5 mM $MgCl_2$, 25 mM KCl, 1 mM DTT, 12 mM 5Hyl, 14 mM ATP-Mg, and 40 μg of AGPHD1. After 3.5 h, the reaction was stopped as above, diluted 3-fold in 10 mM Tris, pH 8.0, and chromatographed on a 3-ml DOWEX AG1X8 column, which was then washed with 3 ml of the same buffer. Assays of P_i (17) before and after hydrolysis with alkaline phosphatase indicated that *5P*Hyl was present in the flow-through and wash fractions and that it was separated from P_i. The yield of this preparation was close to 100% compared with the initial 5Hyl.

Radiochemical Assay of 5PHyl-phospholyase—This assay measures the [P^{32}]P_i production from [^{32}P]*5P*Hyl. The reaction mixture (50 μl) contained 4.5 μg of recombinant human AGXT2L2 (or AGXT2L1) in 20 mM Hepes, pH 7.1, containing 5 μM PLP, 0.5 $mg \cdot ml^{-1}$ bovine serum albumin, 0.15×10^6 cpm [^{32}P]*5P*Hyl and different concentrations of unlabeled *5P*Hyl. After 10 min at 30 °C, the reaction was stopped (5 min at 80 °C), and the samples were centrifuged at 10,000 × *g* for 10 min. [^{32}P]P_i was isolated as a phosphomolybdic complex (18), and its radioactivity was counted.

Assay of Reaction Products of AGXT2L1 and AGXT2L2—AGXT2L1 (0.14 $mg \cdot ml^{-1}$) was incubated at 30 °C in a reaction mixture (0.5 ml) containing 5 mM *P*EtN, 50 mM triethanolamine, pH 7.4, 10 μM PLP, 1 mM EGTA, and 0.5 $mg \cdot ml^{-1}$ bovine serum albumin. AGXT2L2 (0.08 $mg \cdot ml^{-1}$) was incubated in 0.05 ml of a mixture comprising 1 mM *5P*Hyl, 25 mM Hepes, pH 7.1, 10 μM PLP, and 0.5 $mg \cdot ml^{-1}$ bovine serum albumin. In both cases, the reaction was stopped after the indicated time by heating for 5 min at 80 °C. The samples were centrifuged for 10 min at 10,000 × *g* and 4 °C, and the reaction products were measured. Ammonia was assayed spectrophotometrically (19), and P_i was determined in a microplate assay (17). Acetaldehyde was assayed spectrophotometrically by adding yeast alcohol dehydrogenase (final concentration, 0.7 $mg \cdot ml^{-1}$) to a mixture (0.6 ml) containing 50 mM Hepes, pH 7.0, 0.5 $mg \cdot ml^{-1}$ bovine serum albumin, 0.15 mM NADH, and 30 μl of the sample.

The 2-AASA formed in the AGXT2L2 reaction was measured as its dihydroquinazolinium derivative (20) by reverse phase HPLC with a diode array detector at 465 nm. Ten μl of the reaction mixture was mixed with 10 μl of 8 mM *o*-aminobenzaldehyde, incubated for 120 min at 40 °C, and loaded on the column. Quantification was achieved using a standard of allysine ethylene acetal after its hydrolysis in acid conditions.

Assay of Aminotransferase Activity of AGXT2L1 and AGXT2L2—When pyruvate was tested as an amine acceptor, ≈20 μg of AGXT2L1 or AGXT2L2 was incubated at 30 °C in 0.5 ml of a reaction mixture containing 25 mM Hepes, pH 7.2, 25 mM KCl, 1 mM dithiothreitol, 0.5 $mg \cdot ml^{-1}$ bovine serum albumin, 5 μM PLP, 0.02–0.5 mM pyruvate as well as 0, 0.1, or 1 mM β-alanine or β-aminoisobutyrate. The reaction was stopped after 30 min by the addition of $HClO_4$ (5% final concentration). The extract was neutralized with 3 M K_2CO_3 and centrifuged (5 min at 4 °C at 10,000 × *g*). The remaining pyruvate was assayed in the supernatant by computing the change in absorbance at 340 nm following the addition of rabbit muscle lactate dehydrogenase (5 μg) to a 1-ml cuvette containing 20 mM imidazole buffer, pH 7.2, 0.15 mM NADH, and 0.1–0.4 ml of sample. A glutamate dehydrogenase-coupled assay (21) was used to test whether AGXT2L1 or AGXT2L2 catalyzed an aminotransferase reaction between β-alanine, β-aminoisobutyrate (0.1 or 1 mM), L-lysine, L-ornithine, or γ-aminobutyrate (1 or 25 mM) and α-ketoglutarate (0.1 or 2 mM).

Calculations—V_{max} and K_m for the enzymatic activities studied were calculated with Prism 4.0 (GraphPad software) using a nonlinear regression.

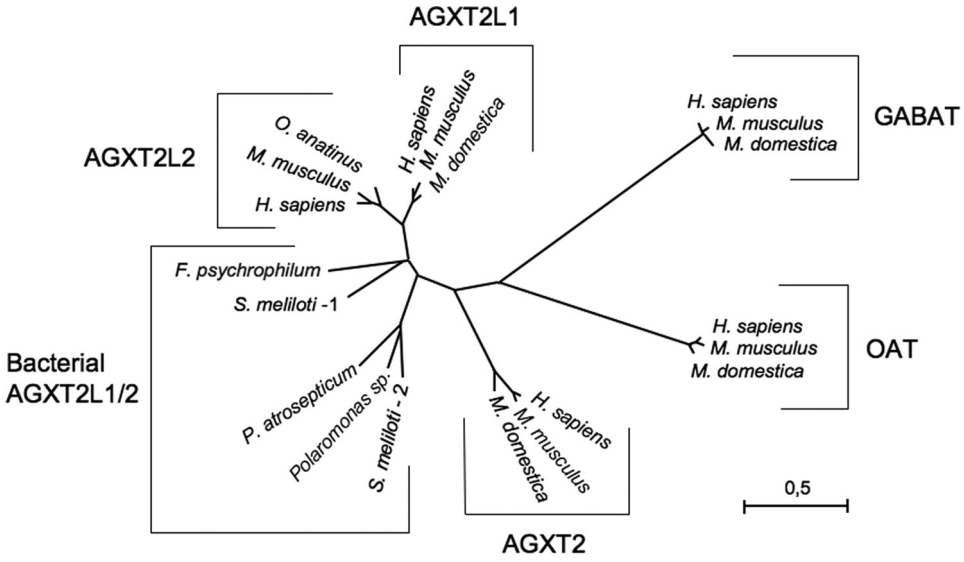

FIGURE 1. **Evolutionary tree of AGXT2L1 and AGXT2L2 and related sequences.** The phylogenetic tree was inferred from the aligned protein sequences using Bayesian analysis (MrBayes) methods. The *horizontal bar* represents 50 substitutions per 100 amino acid residues. The following sequences were used to construct the tree: AGXT2 (alanine-glyoxylate aminotransferase 2) from *Homo sapiens* (NP_114106), *Mus musculus* (Q3UEG6), and *Monodelphis domestica* (XP_001373137); AGXT2L1 (AGXT2-like 1) from *H. sapiens* (NP_112569), *M. musculus* (NP_082183), and *M. domestica* (XP_001364959); AGXT2L2 (AGXT2-like 2) from *H. sapiens* (NP_699204), *M. musculus* (EDL33664), and *Ornithorhynchus anatinus* (XP_001518367); GABAT (γ-aminobutyrate aminotransferase) from *H. sapiens* (NP_065737), *M. musculus* (NP_766549), and *M. domestica* (XP_001376874); ornithine aminotransferase (*OAT*) from *H. sapiens* (NP_000265), *M. musculus* (BAE26718), and *M. domestica* (XP_001363028); bacterial proteins from *Flavobacterium psychrophilum* JIP02/86 (YP_001295781), *P. atrosepticum* SCRI1043 (YP_050155), and *Polaromonas* sp. JS666 (YP_547276); and two proteins from *Sinorhizobium meliloti* 1021 (NP_437638, protein 1; NP_436219, protein 2).

Phylogenetic Analysis—The phylogenetic tree was inferred by maximum likelihood (PhyML, version 3 (22)) for parameter estimation and Bayesian analysis (MrBAYES version 3.1.2 (23)). The Whelan and Goldman model (24) of evolution and a gamma rate distribution parameter of 1.91, with four substitution rate categories, fitted best the data. To estimate Bayesian posterior probabilities, Markov Chain Monte Carlo chains were run for 130,000 generations until convergence and sampled every 100 generations (burn-in: 25,000 generations).

RESULTS

Database Searches—Bi-functional or multi-functional enzymes most often comprise domains that catalyze physiologically related reactions. The identification of a function of an orphan enzyme may therefore be greatly facilitated by the identification of homologues that belong to bi- or multi-functional proteins, if one of the components of these composite proteins has a known function. The existence of close bacterial homologues of an orphan enzyme may also be of great help, because the analysis of operons may point to associations with proteins of known function.

Blast searches performed with AGXT2L1 or AGXT2L2 (which share 67% of identical residues) disclosed the existence of bacterial proteins showing 40–50% identity with either AGXT2L1 or AGXT2L2. This degree of identity is higher than that observed when AGXT2L1 or AGXT2L2 is compared with AGXT2s (≈36% identity), their closest mammalian homologues, suggesting that the bacterial homologues were likely to have a function similar to that of AGXT2L1 or AGXT2L2. The close relationship between AGXT2L1 and AGXT2L2 with bacterial sequences is illustrated in the evolutionary tree represented in Fig. 1. This tree comprises members of five vertebrate proteins belonging to the aminotransferase III family, defined as: AGXT2, AGXT2L1, AGXT2L2, ornithine aminotransferase, and γ-aminobutyrate aminotransferase, in addition to a few selected bacterial homologues of AGXT2L1 and AGXT2L2. The bacterial homologues (bacterial AGXT2L1/2) stem off from the branch leading to AGXT2L1 and AGXT2L2 after the separation between AGXT2 and AGXT2L1 or AGXT2L2 took place.

Remarkably, a significant fraction of the bacterial homologues were putative tri-functional proteins comprising an aminoglycoside phosphotransferase domain and a peptidase M23 domain in addition to the aminotransferase class III domain (as defined in the Pfam database (3)). Other genomes contained shorter bi-functional fusion proteins without the M23 peptidase domain. Additional "bacterial AGXT2L1/2" comprised a single aminotransferase class III domain, but their encoding gene was often close to a gene encoding a protein homologous to the aminoglycoside phosphotransferase found in the putative tri-functional or bi-functional proteins (Fig. 2). This observation strengthened the physiological significance of the association of the putative phosphotransferase (*i.e.* kinase) and the "bacterial AGXT2L1/2."

It should be noted that these aminoglycoside phosphotransferases are very distant from *bona fide* aminoglycoside phosphotransferases, which serve to phosphorylate and inactivate aminoglycoside antibiotics. Interestingly, Blast searches using these putative aminoglycoside phosphotransferases indicated that mammalian genomes encoded a homologous protein named AGPHD1 (aminoglycoside phosphotransferase domain 1) that shared ~26% sequence identity with its bacterial homologues (Fig. 2). These findings suggested that mammalian AGPHD1 was likely to catalyze a reaction that was physiologically connected with the reaction catalyzed by AGXT2L1, AGXT2L2, or both.

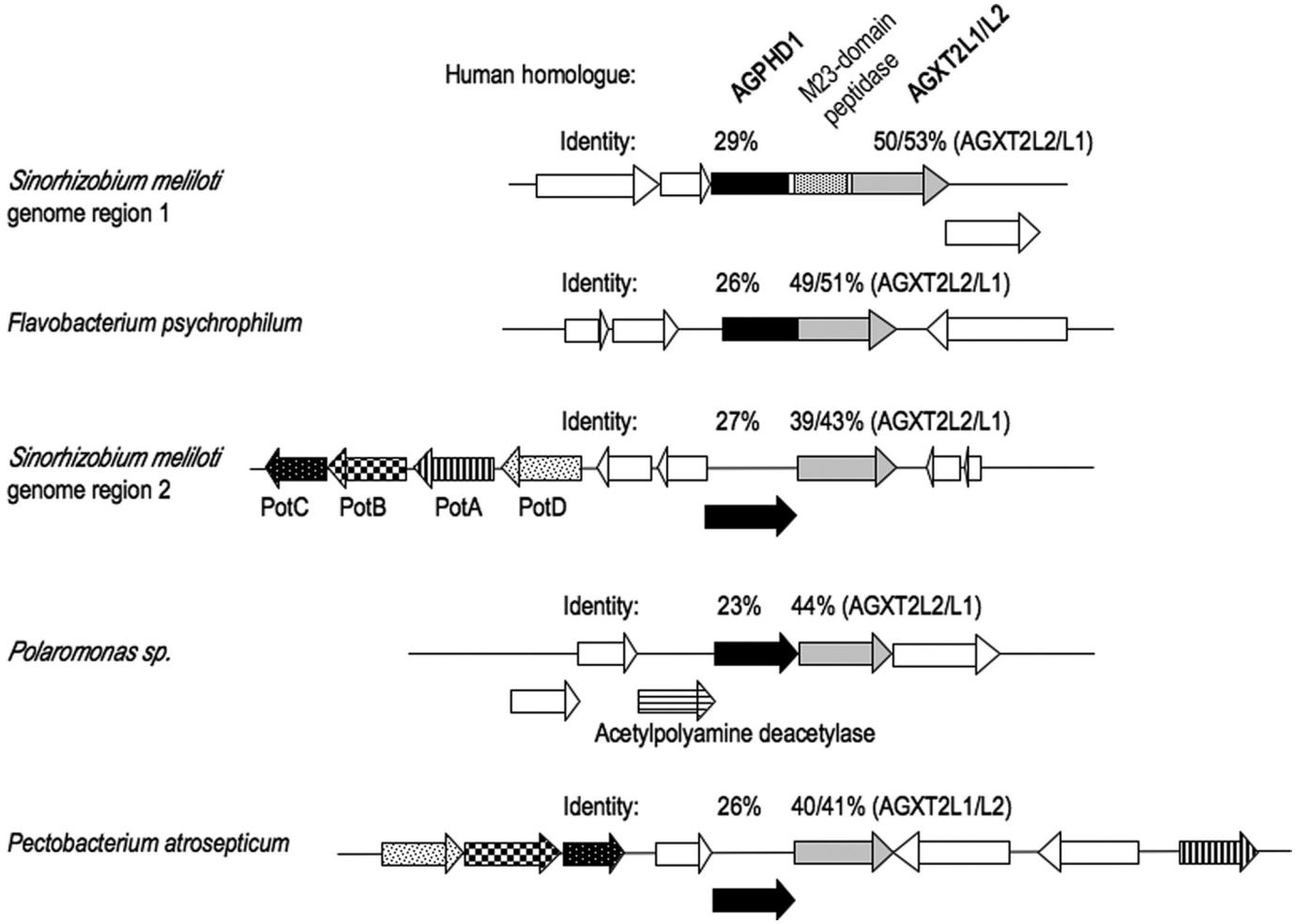

FIGURE 2. **Association of bacterial homologues of AGXT2L1/L2 with putative aminoglycoside phosphotransferases in bacterial genomes.** The figure shows representative examples of the genomic region comprising the bacterial homologues of AGXT2L1/L2 shown in Fig. 1. In some cases, the homologue is a bifunctional protein (YP_001295781) fused with a putative phosphotransferase (as seen in *F. psychrophilum* JIP02/86 contig NC_009613.1) or a trifunctional protein (NP_437638) with an additional putative peptidase of the M23/M37 family ("region 1" of the genome of *S. meliloti* 1021 contig NC_003078). In other cases, it is encoded by a gene neighboring another gene encoding a protein of the aminoglycoside phosphotransferase family (YP_050155 and YP_050154 in *P. atrosepticum* SCRI1043, contig NC_004547.2; YP_547276 and YP_547277 in *Polaromonas* sp. JS666, contig NC_007948.1; and NP_436219 and NP_436218 in region 2 of the genome of *S. meliloti* 1021 contig NC_003037.1). Note in some cases the proximity to genes putatively involved in polyamine metabolism (PotA, PotB, PotC, and PotD, which are different components of the spermidine/putrescine transporter, as well as acetyl-polyamine deacetylase).

According to the Pfam database (24), mammalian AGPHD1 and the homologous bacterial proteins belong to the aminoglycoside phosphotransferase family, which comprises enzymes that phosphorylate aminoglycosides on their third carbon. However, the low degree of identity between human AGPHD1 and its bacterial homologues with authentic aminoglycoside phosphotransferases suggested that AGPHD1 was likely to catalyze the phosphorylation of a substrate different from antibiotics. A common feature of the substrates of the enzymes that belong to the aminoglycoside phosphotransferase family and of the related homoserine kinase and fructosamine kinase families (see Pfam database, family: aminoglycoside phosphotransferase, PF01636) is that they comprise an amino group close to the phosphorylated carbon. Furthermore, our hypothesis that AGPHD1 was functionally linked to enzymes using PLP as a cofactor (*i.e.* AGXT2L1 or AGXT2L2) independently suggested that it catalyzed the phosphorylation of an aminated substrate. Consequently, a literature and database (Expasy-Enzymes; Brenda) search for mammalian enzymes that catalyze the phosphorylation of an aminated substrate that had not yet been molecularly identified led us to consider that AGPHD1 could encode 5Hyl-kinase. Interestingly, the BioGPS database shows that the expression of the AGPHD1 mRNA in mouse tissues is restricted to liver and kidneys, which is consistent with the known tissue distribution of the 5Hyl-kinase activity (25) in support of our hypothesis that AGPHD1 encoded 5Hyl-kinase.

If this hypothesis was correct, we expected that either AGXT2L1 or AGXT2L2 would correspond to the PLP-dependent enzyme that catalyzes the elimination reaction converting 5*P*Hyl to 2-AASA, ammonia and P_i (13). The other of this pair of enzymes would catalyze a similar reaction on *P*EtN, a close structural analogue of C5-C6 of 5*P*Hyl (11). This role of AGXT2L1 and AGXT2L2 is consistent with these proteins being predicted to be cytosolic, which is the localization of both

TABLE 2
Kinetic properties of recombinant human AGPHD1
The results are the means of three determinations ± S.E.

Substrates	V_{max}	K_m	k_{cat}/K_m
	$\mu mol \cdot min^{-1} \cdot mg^{-1}$	μM	$s^{-1} \cdot M^{-1}$
5*R*-5-hydroxy-L-lysine (0–1 mM) + 2 mM ATP	4.95 ± 0.34	280 ± 40	12×10^3
5*R*-5-hydroxy-L-lysine (0–1 mM) + 0.2 mM GTP	0.49 ± 0.01	7.6 ± 0.1	45×10^3
ATP (0–2.5 mM) + 0.5 mM 5*R*-5-hydroxy-L-lysine	5.28 ± 0.20	810 ± 70	5×10^3
GTP (0–25 μM) + 0.5 mM 5*R*-5-hydroxy-L-lysine	0.57 ± 0.03	3.5 ± 1.1	110×10^3

ammoniophospholyases. In the following sections we provide evidence for these assignments.

Characterization of Recombinant Human AGPHD1 as 5Hyl-kinase—Using a spectrophotometric assay monitoring the formation of ADP or GDP, we found that homogeneous recombinant human AGPHD1 with a C-terminal His_6 tag catalyzed the phosphorylation of 5Hyl using either ATP-Mg or GDP-Mg as phosphoryl donors. The substrate saturation curves for 5Hyl were hyperbolic as determined with double reciprocal plots (not shown). AGPHD1 displayed a much higher affinity for GTP-Mg than for ATP-Mg, the K_m being more than 200-fold lower for the former than for the latter nucleotide (Table 2). The V_{max} was, however, ~10-fold higher with ATP-Mg than with GTP-Mg, resulting in a catalytic efficiency that was ≈22-fold higher with GTP-Mg than with ATP-Mg. The K_m for 5Hyl was ~35-fold lower when a near-physiological concentration of GTP-Mg (0.2 mM) was used instead of ATP-Mg (2 mM). No evidence was observed for phosphorylation of ethanolamine, hydroxyproline, homoserine, serine, or choline (all tested at 1 or 5 mM, in the presence of 2 mM ATP-Mg). To check whether the kinase was specific for the physiological form of hydroxylysine, we compared the rate of phosphorylation of 5Hyl with that of a 4-fold higher concentration of a mixture containing all four 5-hydroxy-DL-lysine isomers. In the presence of 1 mM ATP-Mg, the activity of AGPHD1 measured with 50 and 100 μM 5-hydroxy-DL-lysine was ≈1.3- and 1.15-fold higher than that measured with 12.5 and 25 μM 5Hyl, respectively. These findings suggested that the best substrate is the physiological form but that human AGPHD1 can also phosphorylate at a lower rate at least one other isomer.

The availability of purified 5Hyl-kinase allowed us to prepare radioactive and nonradioactive 5*P*Hyl as described under "Experimental Procedures." When chromatographed on an anion exchange resin (DOWEX-AG1X8) in the presence of 10 mM Hepes at pH 7.5, the reaction product behaved as expected for a compound with a partial negative charge. The purified 5*P*Hyl was used to characterize the 5*P*Hyl-phospholyase activity of AGXT2L2.

PEtN-phospholyase Activity of AGXT2L1—We began by determining the *P*EtN-phospholyase activity of purified recombinant human AGXT2L1 and AGXT2L2 by measuring spectrophotometrically the production of acetaldehyde in the presence of 0.5 mM *P*EtN and 10 μM PLP. AGXT2L1 catalyzed this reaction, whereas AGXT2L2 was inactive. At pH 7.4, the K_m of AGXT2L1 for *P*EtN was 680 ± 85 μM, and its V_{max} was 1.46 ± 0.06 $\mu mol \cdot min^{-1} \cdot mg^{-1}$ protein. We also assessed the formation of the other two reaction products, ammonia and P_i. Fig. 3 shows that AGXT2L1 indeed catalyzed the formation of stoichiometric amounts of acetaldehyde, ammonia, and P_i. In these

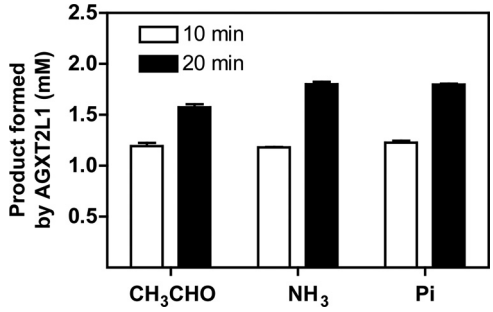

FIGURE 3. **PEtN phospholyase activity of recombinant human AGXT2L1.** AGXT2L1 was incubated with 5 mM *P*EtN for 10 and 20 min at 30 °C, before stopping the reaction. Acetaldehyde (CH_3CHO), ammonia (NH_3), and P_i were measured in the incubation medium.

experiments, the reaction was not linear with time, but this was most likely due to inhibition by P_i, a known inhibitor of rabbit *P*EtN-phospholyase. Inhibition was confirmed in the case of human AGXT2L1: P_i increased the apparent K_m but did not change the V_{max}, consistent with a competitive inhibition. The calculated K_i was 1.2 mM (results not shown), which probably explains the lack of linearity with time observed in the reaction shown in Fig. 3. When PLP was omitted from the reaction mixture, the activity of AGXT2L1 measured with 0.5 mM substrate was reduced to less than 10% of the activity observed in the presence of 10 μM PLP, consistent with PLP being a cofactor of this enzyme. Neither ethanol (20 or 80 mM) nor phosphoserine (0.2, 1 or 5 mM) affected AGXT2L1 activity in the presence of 1 or 5 mM *P*EtN.

5PHyl-phospholyase Activity of AGXT2L2—The *5P*Hyl-phospholyase activity of recombinant human AGXT2L2 and AGXT2L1 was tested through the production of $[^{32}P]P_i$ from $[^{32}P]$5*P*Hyl. AGXT2L2 catalyzed this reaction, whereas AGXT2L1 was inactive, consistent with AGXT2L1 being the *P*EtN-phospholyase. Fig. 4*A* shows that after 30 min of incubation at 30 °C in the presence of 1 mM 5*P*Hyl, AGXT2L2 had formed stoichiometric amounts (≈0.5 mM) of P_i, ammonia, and 2-AASA. The saturation curve of AGXT2L2 for 5*P*Hyl (Fig. 4*B*) suggested that the enzyme was inhibited by excess substrate. A K_m for 5*P*Hyl of 16.9 ± 4.5 μM and a V_{max} of 256 ± 15 $nmol \cdot min^{-1} \cdot mg^{-1}$ protein were computed from the linear portion of double reciprocal plots. In the presence of 0.5 mM 5*P*Hyl, 2, 5, and 10 mM P_i increasingly inhibited the production of ammonia by AGXT2L2. At the highest concentration of P_i, the activity was reduced by 50% (not shown).

Absence of Aminotransferase Activity of AGXT2L1 and AGXT2L2—We also tested the potential aminotransferase activity of purified recombinant AGXT2L1 and AGXT2L2 (with either a N- or a C-terminal His_6 tag) by measuring glutamate formation in incubations containing α-ketoglutarate (0.1

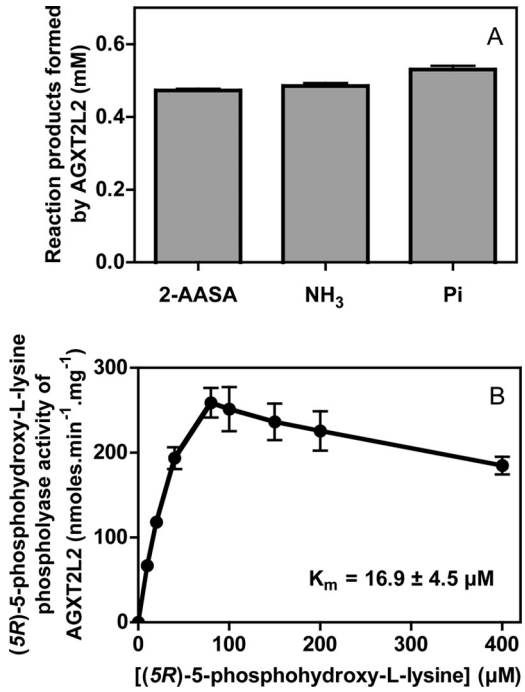

FIGURE 4. **5*P*Hyl phospholyase activity of recombinant human AGXT2L2.** *A*, AGXT2L2 was incubated with 1 mM 5*P*Hyl for 30 min at 30 °C, as described under "Experimental Procedures." After stopping the reaction, 2-AASA, ammonia (NH_3), and P_i were measured in the incubation medium. *B*, the saturation curve of AGXT2L2 was obtained by measuring the production of [^{32}P]P_i from [^{32}P]5*P*Hyl in the presence of variable concentrations of unlabeled 5*P*Hyl.

or 2 mM) as amine acceptor together with β-alanine, β-aminoisobutyrate (0.1 or 1 mM), L-lysine, L-ornithine, or γ-aminobutyrate (1 or 25 mM) as amine donor. We similarly measured pyruvate disappearance in incubations containing pyruvate (0.02, 0.1, or 0.5 mM) as amine acceptor together with β-alanine or β-aminoisobutyrate (0.1 or 1 mM). No aminotransferase activity of AGXT2L1 or AGXT2L2 could be detected in these assays.

DISCUSSION

5Hyl-kinase Is AGPHD1—This identification is supported by the finding that the catalytic activity and the kinetic properties of human recombinant AGPHD1 perfectly agree with the known properties of rat liver 5Hyl-kinase (14). Furthermore, the data on the tissue distribution of the AGPHD1 mRNA (BioGPS database) fit with the knowledge that 5Hyl-kinase activity is primarily present in liver and kidneys. This distribution suggests that 5Hyl-kinase plays a major role in degrading 5Hyl derived from food. Its presence at lower levels in other tissues indicates that it participates also in the catabolism of 5Hyl derived from local collagen breakdown.

The identification of the function of AGPHD1 will allow determination of whether hydroxylysinuria and hydroxylysinemia (26–29) are caused by mutations in its gene. Children and adults with this metabolic abnormality have mental and/or neurological defects, but the clinical picture is not consistent, making it unclear whether the clinical symptoms are really caused by the defect in 5Hyl metabolism. Knowledge of the identity of the 5Hyl-kinase gene will help resolve this question, *e.g.* by identifying additional human subjects with a defect in this enzyme through high throughput genome sequencing approaches.

AGXT2L2 Is 5PHyl-phospholyase—Here also the identification rests on the demonstration that recombinant AGXT2L2 catalyzes the same, PLP-dependent reaction as 5PHyl-phospholyase (13), with similar kinetic properties and tissue distribution (25). 5*P*Hyl-phospholyase is a cytosolic enzyme, which agrees with the predictions made from the sequence of AGXT2L2 both with TargetP (30) and Psort II (31). By contrast, 2-AASA synthase, an enzyme involved in the breakdown of lysine via saccharopine (Fig. 5), is mitochondrial. Thus, 2-AASA is formed both in the cytosol and in mitochondria. Consistent with this, ALDH7A1 (32, 33), the aldehyde dehydrogenase that oxidizes 2-AASA, exists as two isoforms, one mitochondrial and the other cytosolic, which result from the use of alternative in-frame translation initiation codons.

Mutations in the gene encoding AGXT2L2 should give rise to increased urinary excretion of 5*P*Hyl. This condition has only been described in two unrelated patients, both with neurological abnormalities (34). The observation that 5*P*Hyl is a normal constituent of adult brain (35) suggests that this compound may accumulate in this tissue and possibly have detrimental effects on the nervous system if its metabolizing enzyme is deficient. The molecular identification of 5*P*Hyl-phospholyase will help expand the number of observations of a defect in this enzyme and improve our understanding of the pathophysiological mechanisms.

AGXT2L1 Is PEtN-phospholyase—This identification is based on the same arguments as for the two other enzymes. *P*EtN-phospholyase activity is mainly present in the liver and at lower levels in the kidneys of mammals (36), which is in agreement with the data for the expression of mouse AGXT2L1 (BioGPS database). Unlike AGXT2, which is a mitochondrial enzyme, AGXT2L1 is predicted to be in the cytosol, which is also consistent with the subcellular localization observed for *P*EtN-phospholyase.

*P*EtN- and 5*P*Hyl-phospholyases catalyze identical reactions on substrates with similar structures (Fig. 5), and it is therefore not surprising that their sequences are closely related. Remarkably AGXT2L1 has a C-terminal extension of ≈50 residues compared with AGXT2L2. This extension is possibly involved in the regulation of AGXT2L1, either by undergoing a post-translational modification or by forming a (hypothetical) allosteric site. *P*EtN-phospholyase catalyzes indeed a critical reaction, which should be regulated in such a way that *P*EtN, a precursor for phosphatidylethanolamine (37), is maintained at a constant level, ~1 mM in brain (38, 39). Changing this concentration may lead to perturbations in the metabolism of phosphatidylethanolamine, as indicated by the finding that overexpression of mammalian ethanolamine kinase (EKI1) in COS-7 cells increased the intracellular levels of both *P*EtN and phosphaditylethanolamine (6).

AGXT2L1 and Disease—The high level of expression of AGXT2L1 in human brain (BioGPS and the NCBI/GEO profile databases) suggests that this enzyme plays an important role in the metabolism of *P*EtN and in the control of its concentration in the human CNS. It is therefore likely that defects in this enzyme will lead to neurological perturbations.

Phosphoethanolaminuria is often associated with mutations in the gene encoding tissue-nonspecific alkaline phosphatase

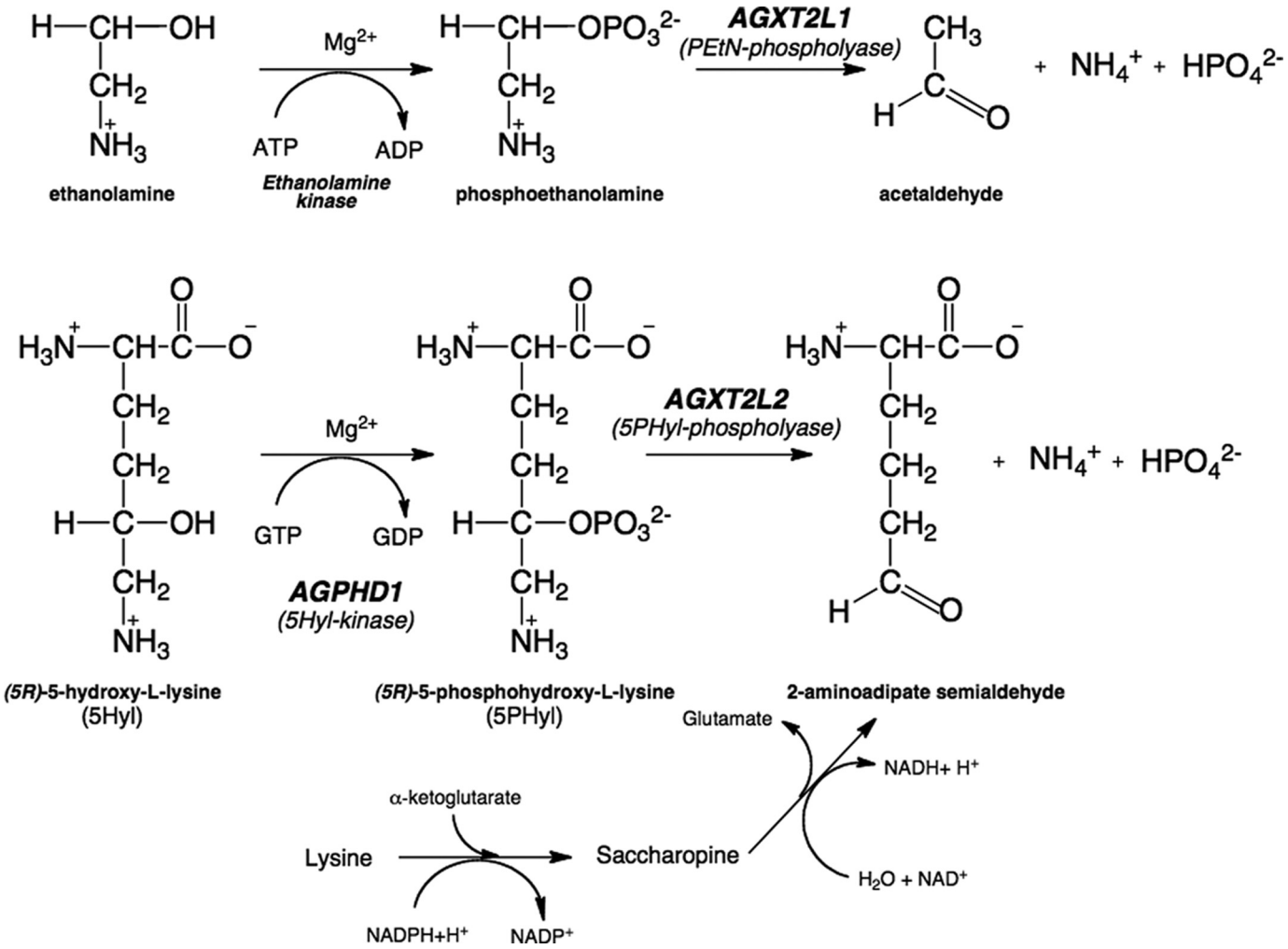

FIGURE 5. **Contribution of AGPHD1, AGXT2L2, and AGXT2L1 to the metabolism of 5*P*Hyl and ethanolamine in vertebrates.**

(40). This enzyme is bound to the cell membrane and cleaves extracellular substrates such as PLP, inorganic pyrophosphate, and *P*EtN. Thus, AGXT2L1 deficiency is likely to lead to ethanolaminuria rather than phosphoethanolaminuria. Ethanolaminuria is likely to be caused also by ethanolamine kinase deficiency. There are few reports of ethanolaminuria (41–44), and its significance is not known. The variability in the associated symptoms (often including neurological symptoms) and in the amount of ethanolamine excreted in urine suggests that different genetic defects may be involved.

In addition to this, several studies suggest that AGXT2L1 may be involved in psychiatric disorders. AGXT2L1 was reported to be among the most up-regulated brain-specific genes in bipolar disorder and schizophrenia (45). AGXT2L1 was down-regulated in suicide completers (46) and in 72% of major depressive disorder: suicide cases compared with age-matched controls (47). A genome-wide association analysis indicated the association of schizophrenia with SNPs in the region of the COL25A1 gene, near the AGXT2L1 gene, on chromosome 4q25 (48). AGXT2L1 was the most up-regulated gene in a genome-wide expression study following 2 weeks of lithium administration to mice (49). With the identification of AGXT2L1 as the *P*EtN catabolic enzyme (and not as a transaminase participating in glutamate catabolism [50]), these findings suggest that the pathophysiology of schizophrenia and bipolar disorder may involve a perturbation in *P*EtN metabolism. Although it is difficult to formulate a coherent hypothesis at this stage, this conclusion is consistent with the finding that the *P*EtN and glycerophosphorylethanolamine levels, as determined by ^{31}P magnetic resonance spectroscopy, are increased in the brain of chronic, medicated schizophrenic compared with matched controls (39).

Function of Bacterial Homologues of Vertebrate AGPHD1 and AGXT2L1/2—The role of the bacterial homologues of AGXT2L1/2 and AGPHD1 is unclear at this stage. *E. carotovora* (*P. atrosepticum* in Fig. 2) has two different loci comprising each an AGXT2L1/2 homologue and an AGPHD1 homologue. It is likely that one or both of these pairs of enzymes are involved in the conversion of ethanolamine to acetaldehyde that has been reported previously (12). However, the fact that ethanolamine metabolism did not proceed further than its conversion to acetaldehyde because of the lack of acetaldehyde dehydrogenase suggests that the physiological function of these enzymes in this bacterium must be in the metabolism of a compound different from ethanolamine. The absence of an aminoadipate semialdehyde dehydrogenase orthologue from the *E.*

carotovora genome[4] argues against 5Hyl being the physiological substrate.

A candidate that needs to be taken into consideration, at least in some bacteria, is 2-hydroxyputrescine, a major polyamine in some prokaryotes (51). Because this compound has a hydroxyl group that neighbors an amine, it may be metabolized by phosphorylation followed by ammoniophospholysis, which would lead to the formation of aminobutyraldehyde. Interestingly, the genome of *Conexibacter woesei* DSM 14684 comprises a gene encoding a "trifunctional protein" next to a gene encoding a putative 4-aminobutyraldehyde dehydrogenase.[4] Furthermore, in two of the genomes shown in Fig. 2, the AGXT2L1/2 and AGPHD1 bacterial homologues are encoded by genes that are close to operons involved in polyamine transport. These enzymes could therefore be involved in the metabolism of 2-hydroxyputrescine in prokaryotes.

Acknowledgment—We thank Prof. Frederick Opperdoes for advice on the phylogenetic analysis.

REFERENCES

1. Percudani, R., and Peracchi, A. (2003) A genomic overview of pyridoxal-phosphate-dependent enzymes. *EMBO Rep.* **4,** 850–854
2. Percudani, R., and Peracchi, A. (2009) The B6 database. A tool for the description and classification of vitamin B_6-dependent enzymatic activities and of the corresponding protein families. *BMC Bioinformatics* **10:** 273
3. Finn, R. D., Mistry, J., Tate, J., Coggill, P., Heger, A., Pollington, J. E., Gavin, O. L., Gunasekaran, P., Ceric, G., Forslund, K., Holm, L., Sonnhammer, E. L., Eddy, S. R., and Bateman, A. (2010) The Pfam protein families database. *Nucleic Acids Res.* **38,** D211–D222
4. Tamaki, N., Sakata, S. F., and Matsuda, K. (2000) Purification, properties, and sequencing of aminoisobutyrate aminotransferases from rat liver. *Methods Enzymol.* **324,** 376–389
5. Donini, S., Ferrari, M., Fedeli, C., Faini, M., Lamberto, I., Marletta, A. S., Mellini, L., Panini, M., Percudani, R., Pollegioni, L., Caldinelli, L., Petrucco, S., and Peracchi, A. (2009) Recombinant production of eight human cytosolic aminotransferases and assessment of their potential involvement in glyoxylate metabolism. *Biochem. J.* **422,** 265–272
6. Lykidis, A., Wang, J., Karim, M. A., and Jackowski, S. (2001) Overexpression of a mammalian ethanolamine-specific kinase accelerates the CDP-ethanolamine pathway. *J. Biol. Chem.* **276,** 2174–2179
7. Tian, Y., Jackson, P., Gunter, C., Wang, J., Rock, C. O., and Jackowski, S. (2006) Placental thrombosis and spontaneous fetal death in mice deficient in ethanolamine kinase 2. *J. Biol. Chem.* **281,** 28438–28449
8. Kiss, Z. (1992) The long-term combined stimulatory effects of ethanol and phorbol ester on phosphatidylethanolamine hydrolysis are mediated by a phospholipase C and prevented by overexpressed α-protein kinase C in fibroblasts. *Eur. J. Biochem.* **209,** 467–473
9. Kiss, Z., and Garamszegi, N. (1993) Overexpression of protein kinase C-epsilon enhances the stimulatory effect of ethanol on phospholipase C-mediated hydrolysis of phosphatidylethanolamine in NIH 3T3 fibroblasts. *FEBS Lett.* **333,** 229–232
10. Stoffel, W., LeKim, D., and Sticht, G. (1969) Distribution and properties of dihydrosphingosine-1-phosphate aldolase (sphinganine-1-phosphate alkanal-lyase). *Hoppe-Seylers Z. Physiol. Chem.* **350,** 1233–1241
11. Fleshood, H. L., and Pitot, H. C. (1970) The metabolism of *O*-phosphorylethanolamine in animal tissues. I. *O*-Phosphorylethanolamine phospho-lyase. Partial purification and characterization. *J. Biol. Chem.* **245,** 4414–4420
12. Jones, A., Faulkner, A., and Turner, J. M. (1973) Microbial metabolism of amino alcohols. Metabolism of ethanolamine and 1-aminopropan-2-ol in species of *Erwinia* and the roles of amino alcohol kinase and amino alcohol *o*-phosphate phospho-lyase in aldehyde formation. *Biochem. J.* **134,** 959–968
13. Tsai, C. H., and Henderson, L. M. (1974) Degradation of *O*-phosphohydroxylysine by rat liver. Purification of the phospho-lyase. *J. Biol. Chem.* **249,** 5784–5789
14. Hiles, R. A., and Henderson, L. M. (1972) The partial purification and properties of hydroxylysine kinase from rat liver. *J. Biol. Chem.* **247,** 646–651
15. Maliekal, P., Vertommen, D., Delpierre, G., and Van Schaftingen, E. (2006) Identification of the sequence encoding *N*-acetylneuraminate-9-phosphate phosphatase. *Glycobiology* **16,** 165–172
16. Veiga-da-Cunha, M., Sokolova, T., Opperdoes, F., and Van Schaftingen, E. (2009) Evolution of vertebrate glucokinase regulatory protein from a bacterial *N*-acetylmuramate 6-phosphate etherase. *Biochem. J.* **423,** 323–332
17. Itaya, K., and Ui, M. (1966) A new micromethod for the colorimetric determination of inorganic phosphate. *Clin. Chim. Acta* **14,** 361–366
18. McClard, R. W. (1979) Synthesis and purification of [1-^{32}P]fructose-1,6-bisophosphate with high specific radioactivity. *Anal. Biochem.* **96,** 500–503
19. Bergmeyer, H.-U., and Beutler, H.-O. (1990) Ammonia, in *Methods of Enzymatic Analysis* (Bergmeyer, H. U., ed) Vol. VIII, 3rd Ed., pp. 454–461, VCH, New York
20. Soda, K., Misono, H., and Yamamoto, T. (1968) L-Lysine:α-ketoglutarate aminotransferase. I. Identification of a product, Δ-1-piperideine-6-carboxylic acid. *Biochemistry* **7,** 4102–4109
21. Beutler, H.-O. (1990) L-Glutamate, colorimetric method with glutamate dehydrogenase and diaphorase, in *Methods of Enzymatic Analysis* (Bergmeyer, H. U., ed) Vol. VIII, pp. 369–376, 3rd Ed., VCH, New York
22. Guindon, S., and Gascuel, O. (2003) A simple, fast, and accurate algorithm to estimate large phylogenies by maximum likelihood. *Syst. Biol.* **52,** 696–704
23. Huelsenbeck, J. P., and Ronquist, F. (2001) MRBAYES. Bayesian inference of phylogenetic trees. *Bioinformatics* **17,** 754–755
24. Whelan, S., and Goldman, N. (2001) A general empirical model of protein evolution derived from multiple protein families using a maximum-likelihood approach. *Mol. Biol. Evol.* **18,** 691–699
25. Hiles, R. A., Willett, C. J., and Henderson, L. M. (1972) Hydroxylysine metabolism in rats, mice, and chickens. *J. Nutr.* **102,** 195–203
26. Parker, C. E., Shaw, K. N. F., Jacobs, E. E., and Gutenstein, M. (1970) Hydroxylysinuria. *Lancet* **295,** 1119–1120
27. Hoefnagel, D., and Pomeroy, J. (1970) Hydroxylysinuria. *Lancet* **760,** 1342–1343
28. Goodman, S. I., Browder, J. A., Hiles, R. A., and Miles, E. S. (1972) Hydroxylysinemia. A disorder due to a defect in the metabolism of free hydroxylysine. *Biochem. Med.* **6,** 344–354
29. Benson, P. F., Swift, P. N., and Young, V. K. (1969) Hydroxylysinuria. *Arch. Dis. Child.* **44,** 134–135
30. Emanuelsson, O., Brunak, S., von Heijne, G., and Nielsen, H. (2007) Locating proteins in the cell using TargetP, SignalP and related tools. *Nat. Protoc.* **2,** 953–971
31. Nakai, K., and Kanehisa, M. (1992) A knowledge base for predicting protein localization sites in eukaryotic cells. *Genomics* **14,** 897–911
32. Tsai, C. H., and Henderson, L. M. (1974) Degradation of *O*-phosphohydroxylysine in rat liver. Purification and properties of 2-aminoadipic semialdehyde dehydrogenase. *J. Biol. Chem.* **249,** 5790–5792
33. Brocker, C., Lassen, N., Estey, T., Pappa, A., Cantore, M., Orlova, V. V., Chavakis, T., Kavanagh, K. L., Oppermann, U., and Vasiliou, V. (2010) Aldehyde dehydrogenase 7A1 (ALDH7A1) is a novel enzyme involved in cellular defense against hyperosmotic stress. *J. Biol. Chem.* **285,** 18452–18463
34. Dorland, L., Duran, M., de Bree, P. K., Smith, G. R., Horvath, A., Tibosch, A. S., and Wadman, S. K. (1990) O-phosphohydroxylysinuria. A new inborn error of metabolism? *Clin. Chim. Acta* **188,** 221–226
35. Astrup, T., Carlstrom, G., and Stage, A. (1951) Free amino acids in mammalian tissue. *Acta Physiol. Scand.* **24,** 202–211
36. Fleshood, H. L., and Pitot, H. C. (1970) The metabolism of *O*-phospho-

[4] M. Veiga-da-Cunha and E. Van Schaftingen, unpublished observations.

rylethanolamine in animal tissues. II. Metabolic regulation of *O*-phosphorylethanolamine phospho-lyase *in vivo*. *Arch. Biochem. Biophys.* **141,** 423–429
37. Vance, J. E. (2008) Phosphatidylserine and phosphatidylethanolamine in mammalian cells. Two metabolically related aminophospholipids. *J. Lipid Res.* **49,** 1377–1387
38. Ansell, G. B., and Richter, D. (1954) A note on the free amino acid content of rat brain. *Biochem. J.* **57,** 70–73
39. Jensen, J. E., Al-Semaan, Y. M., Williamson, P. C., Neufeld, R. W., Menon, R. S., Schaeffer, B., Densmore, M., and Drost, D. J. (2002) Region-specific changes in phospholipid metabolism in chronic, medicated schizophrenia. ^{31}P-MRS study at 4.0 Tesla. *Br. J. Psychiatry* **180,** 39–44
40. Fedde, K. N., and Whyte, M. P. (1990) Alkaline phosphatase (tissue-nonspecific isoenzyme) is a phosphoethanolamine and pyridoxal-5′-phosphate ectophosphatase. Normal and hypophosphatasia fibroblast study. *Am. J. Hum. Genet.* **47,** 767–775
41. Vietor, K. W., Havsteen, B., Harms, D., Busse, H., and Heyne, K. (1977) Ethanolaminosis. A newly recognized, generalized storage disease with cardiomegaly, cerebral dysfunction and early death. *Eur. J. Pediatr.* **126,** 61–75
42. Wijburg, H., de Jong, J., Wevers, R., Bakkeren, J., Trijbels, F., and Sengers, R. (1992) Beta-mannosidosis and ethanolaminuria in a female patient. *Eur. J. Pediatr.* **151,** 311
43. Dent, C. E., and Walshe, J. M. (1953) Primary carcinoma of the liver. Description of a case with ethanolaminuria, a new and obscure metabolic defect. *Br. J. Cancer* **7,** 166–180
44. Cole, D. E., Farag, S., and Dooley, K. C. (1988) Ethanolaminuria. A non-specific laboratory finding in the seriously ill infant. *Clin. Biochem.* **21,** 297–300
45. Shao, L., and Vawter, M. P. (2008) Shared gene expression alterations in schizophrenia and bipolar disorder. *Biol. Psychiatry* **64,** 89–97
46. Kim, S., Choi, K. H., Baykiz, A. F., and Gershenfeld, H. K. (2007) Suicide candidate genes associated with bipolar disorder and schizophrenia. An exploratory gene expression profiling analysis of post-mortem prefrontal cortex. *BMC Genomics* **8,** 413
47. Sibille, E., Arango, V., Galfalvy, H. C., Pavlidis, P., Erraji-Benchekroun, L., Ellis, S. P., and John Mann, J. (2004) Gene expression profiling of depression and suicide in human prefrontal cortex. *Neuropsychopharmacology* **29,** 351–361
48. Wang, K. S., Liu, X., Zhang, Q., Aragam, N., and Pan, Y. (2011) Genome-wide association analysis of age at onset in schizophrenia in a European-American sample. *Am. J. Med. Genet. B. Neuropsychiatr. Genet.* **156B,** 671–680
49. McQuillin, A., Rizig, M., and Gurling, H. M. (2007) A microarray gene expression study of the molecular pharmacology of lithium carbonate on mouse brain mRNA to understand the neurobiology of mood stabilization and treatment of bipolar affective disorder. *Pharmacogenet. Genomics* **17,** 605–617
50. Altar, C. A., Vawter, M. P., and Ginsberg, S. D. (2009) Target identification for CNS diseases by transcriptional profiling. *Neuropsychopharmacology* **34,** 18–54
51. Hamana, K. (1997) Polyamine distribution patterns within the families Aeromonadaceae, Vibrionaceae, Pasteurellaceae, and Halomonadaceae, and related genera of the gamma subclass of the Proteobacteria. *J. Gen. Appl. Microbiol.* **43,** 49–59